This is the published version of:

The final publication is available at http://dx.doi.org/10.1515/cls-2015-0001

When citing this work, cite the original published paper.

DE GRUYTER OPEN

Curved and Layer. Struct. 2015; 2:1–14

Amir Hossein Mohazzab and Lorenzo Dozio*

Prediction of natural frequencies of laminated curved panels using refined 2-D theories in the spectral collocation method

Abstract: This paper presents a versatile and efficient modeling and solution framework for free vibration analysis of composite laminated cylindrical and spherical panels modeled according to two-dimensional equivalent single-layer and layerwise theories of variable order. A unified formulation of the equations of motion is adopted which can be used for both thin and thick structures. The discretization procedure is based on the spectral collocation method and is presented in a compact matrix form which can be directly and easily implemented. The convergence and accuracy of the proposed approach is evaluated for panels having different boundary conditions, thickness and shallowness ratios, and lamination layups.

1 Introduction

Accurate yet efficient modeling and solution of shell structures can be considered a classical problem in structural mechanics [1–4]. Over the last 50 years, researchers proposed many different approaches to face this problem [5–7], urged by the increasing adoption of curved panels as structural elements in a large variety of engineering applications. For example, cylindrical and spherical panels are important components of built-up aircraft and spacecraft structures. Shell structures are also widely applied in automotive, marine and civil engineering disciplines. In the last three decades, the design of shell structures has known new exciting opportunities by the usage of composite materials [8, 9]. Composite laminated shells offer higher stiffness/strength to weight ratios than most metallic constructions and today they are fairly common in advanced engineering applications such as aerospace systems.

In service, such curved laminated panels are typically subjected to various dynamic loads, and it is crucial that their dynamic response is well predicted from the design stage onwards in order to assure their integrity and stability. One of the most important purpose in any linear dynamic analysis is the accurate computation of the natural frequencies of the system [10, 11]. Broadly speaking, the accuracy of free vibration analysis of laminated shells mainly relies on two aspects. The first issue is related to the assumptions and simplifications adopted in the mathematical model of the structural component. The second aspect involves the method selected to solve the governing equations of the problem. A brief discussion of both aspects follows.

Models of curved panels based upon the three dimensional (3-D) theory of elasticity can be considered as the most accurate, since no overly simplified assumptions are introduced in describing the kinematics of deformations [12–15]. As such, 3-D models are suitable for shells of any thickness ratio (defined as the ratio between the thickness of the panel to the shortest of the span lengths or radii of curvature) and any shallowness ratio (defined as the ratio of the shortest span length to one of the radii of curvature), ranging from thin and shallow to thick and deep shells vibrating at low to high frequency. However, a full 3-D dynamic analysis, especially for composite shells, is rather complicated and time consuming. Therefore, so-called shell theories aimed at reducing the problem from three to two dimensions have been introduced by employing appropriate assumptions on the displacement behavior in the thickness direction.

Many different displacement-based two-dimensional (2-D) theories for laminated curved panels are available

*Corresponding Author: Lorenzo Dozio:** Department of Aerospace Science and Technology, Politecnico di Milano, via La Masa, 34, 20156, Milan, Italy
Amir Hossein Mohazzab: Department of Aerospace Science and Technology, Politecnico di Milano, via La Masa, 34, 20156, Milan, Italy

and a review of the extensive literature on this topic is beyond the scope of the present work [9]. Generally speaking, we can distinguish between equivalent single-layer (ESL) and layerwise (LW) theories [16], including or not shear deformation, rotary inertia and thickness stretching factors. ESL approaches assume a proper overall kinematic field throughout the thickness of the laminated structure, whereas an independent displacement field is postulated for each layer in a LW framework and appropriate continuity conditions are imposed at each layer interface. Typically, both ESL and LW kinematic fields are expressed as complete polynomial series expansion of the thickness coordinate and the highest power of the assumed polynomial set is generally referred to as the order of the theory. Owing to their intrinsic simplifications, 2-D theories provide reliable models for a limited range of thickness ratios, frequency values and through-the-thickness variation of material properties. The accuracy usually degrades as the wavelength of the vibration mode is of the order of magnitude of the panel thickness and as the variation of mechanical properties through the thickness direction increases like the case of sandwich panels. This loss of accuracy can be successfully compensated by using theories of higher order and/or relying on a LW approach, with the price of increasing the complexity and computational cost of the resulting models. Frequently, the knowledge in advance of the correct shell theory balancing the accuracy and computational burden for the specific problem under investigation can be a hard task. A unified modeling framework capable of tailoring the order and typology of the shell theory without the need of a new modeling effort each time would be highly desirable.

The other important aspect related to the computation of natural frequencies of laminated curved panels is the method adopted to solve the equations governing the dynamic problem. Again, many different approaches are available in the literature [9]. Exact solutions satisfying both the differential equations and the boundary conditions are possible only for a limited set of shell geometries, boundary conditions and lamination sequences. In most practical situations, one must rely on approximate methods. The most common and traditional approaches include the Ritz method and the finite element method (FEM). For simple structures, the Ritz method shows better convergence and less computational need than FEM. However, the FEM overcomes the limitations of the Ritz method in dealing with complicated boundary conditions and complex shapes. More recently, new emerging meshless methods are increasingly applied to the analysis of shell problems with the aim of eliminating some difficulties existing in FEM such as mesh distortion and remeshing [17]. Among recent solution methods, the generalized differential quadrature (GDQ) is also attracting more and more interest due to its simplicity and versatility [18–20].

The scope of this work is to present an advanced modeling and solution framework for the free vibration analysis of both thin and thick, deep and shallow laminated cylindrical and spherical panels with different combinations of boundary conditions. The range of applicability of the resulting tool is similar to a fully 3-D analysis, with also the possibility of using economical low-order theories when more refined models are not required. Therefore, the balance between accuracy and computational savings can be tailored on the specific application under study. The modeling aspect exploits the power and versatility of the unified formulation proposed by Carrera [21], which provides a smart way of handling arbitrary refinements of classical shell theories. The discretization of the problem to obtain an approximate solution of the natural frequencies is performed by the spectral collocation method, also called pseudospectral method [22, 23], which is known to exhibit high rate of convergence and accuracy for differential problems without singularities. In so doing, relatively light discretized models are obtained which can be profitably used in extensive optimization and parametric studies.

As a final remark, it is noted that recent papers with some similarities with the present approach are available in the literature. In particular, worth mentioning are the works of [20], [24] and [25]. The first reference contains a comprehensive study of free vibrations of eight different shell structures using the GDQ method. The work is highly insightful but it is limited to models based on ESL theories. The paper by [24] applies a radial basis functions collocation method to perform a static and free vibration analysis of cylindrical and spherical laminated panels. Although the approximation of the problem is different, the discretization procedure is quite similar to what presented here. However, the analysis has the limitation of considering only models based on a first-order layerwise theory. Finally, the work reported in [25] uses a hierarchical trigonometric Ritz method to compute the natural frequencies of laminated shells. The approach is similar to that provided by [26–28] and can rely on both ESL and LW models of variable order. However, the analysis in the paper by [25] considers only panels having fully simply-supported edges. This work aims at overcoming the limitations of the above references by considering a comprehensive set of both ESL and LW shell theories of different orders and studying laminated panels with various combinations of classical boundary conditions.
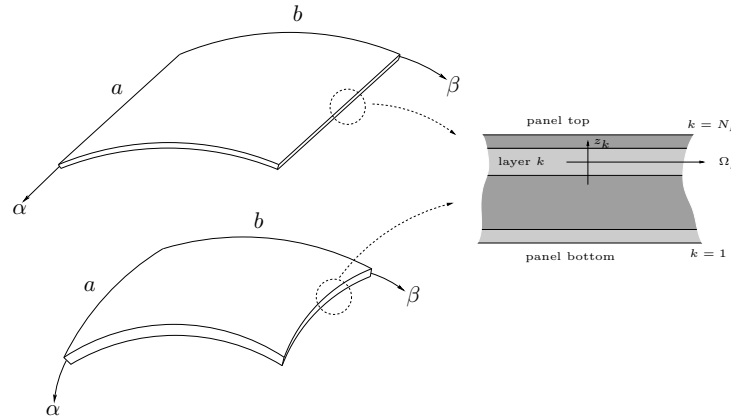
Figure 1: Geometry of the multilayered cylindrical and spherical panels considered in this work and details of the lamination lay-up.

2 Modeling framework

Let's consider the cylindrical and spherical laminated panels in Figure 1, which are composed of N_ℓ layers of homogeneous orthotropic material. Each layer k has thickness h_k and is numbered sequentially from bottom ($k = 1$) to top ($k = N_\ell$) of the panel. The total thickness of the panel is $h = \sum_{k=1}^{N_\ell} h_k$. The undeformed middle surface Ω_k of each layer is described by the two orthogonal curvilinear coordinates α and β. Let z_k denote the rectilinear local thickness coordinate in the normal direction with respect to Ω_k. The components of the displacement field of layer k are indicated as u_α^k, u_β^k and u_z^k in the α, β and z directions, respectively.

According to 3-D elasticity and considering curved panels with constant curvature, the in-plane strains $\boldsymbol{\varepsilon}_p^k = \left\{ \begin{array}{ccc} \varepsilon_{\alpha\alpha}^k & \varepsilon_{\beta\beta}^k & \gamma_{\alpha\beta}^k \end{array} \right\}^T$ of the layer k can be expressed as a function of the displacement components $\mathbf{u}^k = \left\{ \begin{array}{ccc} u_\alpha^k & u_\beta^k & u_z^k \end{array} \right\}^T$ by the following relation:

$$\boldsymbol{\varepsilon}_p^k = \left(\mathcal{D}_p^k + \mathcal{A}_p^k \right) \mathbf{u}^k \tag{1}$$

where

$$\mathcal{D}_p^k = \begin{bmatrix} \frac{1}{H_\alpha^k} \frac{\partial}{\partial \alpha} & 0 & 0 \\ 0 & \frac{1}{H_\beta^k} \frac{\partial}{\partial \beta} & 0 \\ \frac{1}{H_\beta^k} \frac{\partial}{\partial \beta} & \frac{1}{H_\alpha^k} \frac{\partial}{\partial \alpha} & 0 \end{bmatrix} \qquad \mathcal{A}_p^k = \begin{bmatrix} 0 & 0 & \frac{1}{H_\alpha^k R_\alpha^k} \\ 0 & 0 & \frac{1}{H_\beta^k R_\beta^k} \\ 0 & 0 & 0 \end{bmatrix} \tag{2}$$

R_α^k and R_β^k are the curvature radii of the α and β coordinate curves, respectively, at the generic point of the middle surface Ω_k of the layer, and

$$H_\alpha^k = 1 + \frac{z_k}{R_\alpha^k} \qquad H_\beta^k = 1 + \frac{z_k}{R_\beta^k} \tag{3}$$

It is noted that $H_\alpha^k = 1$ for cylindrical panels since $R_\alpha^k = \infty$ and $H_\alpha^k = H_\beta^k$ for spherical panels since $R_\alpha^k = R_\beta^k$. Note also

that when $1/R_\alpha^k = 1/R_\beta^k = 0$, the above relations degenerate to those for plates.

Similarly, the normal strain components $\boldsymbol{\varepsilon}_n^k = \left\{ \begin{array}{ccc} \gamma_{\alpha z}^k & \gamma_{\beta z}^k & \varepsilon_{zz}^k \end{array} \right\}^T$ can be expressed as follows

$$\boldsymbol{\varepsilon}_n^k = \left(\mathcal{D}_n^k - \mathcal{A}_n^k + \mathcal{D}_z^k \right) \mathbf{u}^k \tag{4}$$

where

$$\mathcal{D}_n^k = \begin{bmatrix} 0 & 0 & \frac{1}{H_\alpha^k} \frac{\partial}{\partial \alpha} \\ 0 & 0 & \frac{1}{H_\beta^k} \frac{\partial}{\partial \beta} \\ 0 & 0 & 0 \end{bmatrix} \qquad \mathcal{A}_n^k = \begin{bmatrix} \frac{1}{H_\alpha^k R_\alpha^k} & 0 & 0 \\ 0 & \frac{1}{H_\beta^k R_\beta^k} & 0 \\ 0 & 0 & 0 \end{bmatrix} \tag{5}$$

and $\mathcal{D}_z^k = \frac{\partial}{\partial z} \mathbf{I}_3$.

Assuming a linearly elastic orthotropic material, the constitutive equations of the kth layer in the laminate reference coordinate system are written as

$$\begin{aligned} \boldsymbol{\sigma}_p^k &= \tilde{\mathbf{C}}_{pp}^k \boldsymbol{\varepsilon}_p^k + \tilde{\mathbf{C}}_{pn}^k \boldsymbol{\varepsilon}_n^k \\ \boldsymbol{\sigma}_n^k &= \tilde{\mathbf{C}}_{pn}^{k^T} \boldsymbol{\varepsilon}_p^k + \tilde{\mathbf{C}}_{nn}^k \boldsymbol{\varepsilon}_n^k \end{aligned} \tag{6}$$

where $\boldsymbol{\sigma}_p^k = \left\{ \begin{array}{ccc} \sigma_{\alpha\alpha}^k & \sigma_{\beta\beta}^k & \tau_{\alpha\beta}^k \end{array} \right\}^T$ is the vector of in-plane stresses, $\boldsymbol{\sigma}_n^k = \left\{ \begin{array}{ccc} \tau_{\alpha z}^k & \tau_{\beta z}^k & \sigma_{zz}^k \end{array} \right\}^T$ is the vector of normal stresses, and the matrices of stiffness coefficients given by

$$\tilde{\mathbf{C}}_{pp}^k = \begin{bmatrix} \tilde{C}_{11}^k & \tilde{C}_{12}^k & \tilde{C}_{16}^k \\ \tilde{C}_{12}^k & \tilde{C}_{22}^k & \tilde{C}_{26}^k \\ \tilde{C}_{16}^k & \tilde{C}_{26}^k & \tilde{C}_{66}^k \end{bmatrix} \qquad \tilde{\mathbf{C}}_{pn}^k = \begin{bmatrix} 0 & 0 & \tilde{C}_{13}^k \\ 0 & 0 & \tilde{C}_{23}^k \\ 0 & 0 & \tilde{C}_{36}^k \end{bmatrix} \tag{7}$$

$$\tilde{\mathbf{C}}_{nn}^k = \begin{bmatrix} \tilde{C}_{55}^k & \tilde{C}_{45}^k & 0 \\ \tilde{C}_{45}^k & \tilde{C}_{44}^k & 0 \\ 0 & 0 & \tilde{C}_{33}^k \end{bmatrix} \tag{8}$$

are derived from those expressed in the layer reference system through a proper coordinate transformation [29].

Within the modeling framework proposed by Carrera [21], an entire class of 2-D shell theories can be employed by expressing the displacement vector $\mathbf{u}^k$ through the Einstein notation as follows

$$\mathbf{u}^k(\alpha, \beta, \zeta_k, t) = F_\tau(\zeta_k)\mathbf{u}_\tau^k(\alpha, \beta, t) \tag{9}$$

where $\zeta_k = 2z_k/h_k$ is the dimensionless thickness coordinate of the layer ($-1 \le \zeta_k \le 1$), τ is the theory-related index, $F_\tau(\zeta_k)$ are appropriate thickness functions defined locally for each layer, and

$$\mathbf{u}_\tau^k(\alpha, \beta, t) = \left\{ \begin{array}{c} u_{\alpha\tau}^k(\alpha, \beta, t) \\ u_{\beta\tau}^k(\alpha, \beta, t) \\ u_{z\tau}^k(\alpha, \beta, t) \end{array} \right\} \tag{10}$$

is the vector of generalized kinematic coordinates in the assumed displacement model corresponding to index τ. Various ESL and LW theories of different order, which is a free parameter of the formulation, can be obtained by choosing the type of thickness functions and the range values of τ in Eq. (9). Both a class of LW theories and a class of ESL theories are implemented in this work. They are briefly presented in the following.

A family of LW theories of variable order N is considered by assuming $\tau = t, b, r$ ($r = 2, \ldots, N$) and selecting

$$
\begin{aligned}
F_t(\zeta_k) &= \frac{1 + \zeta_k}{2} \\
F_b(\zeta_k) &= \frac{1 - \zeta_k}{2} \\
F_r(\zeta_k) &= P_r(\zeta_k) - P_{r-2}(\zeta_k)
\end{aligned}
\tag{11}
$$

where $P_r(\zeta_k)$ is the Legendre polynomial of rth order. In so doing, the displacement variables $\mathbf{u}_b^k$ and $\mathbf{u}_t^k$ are the actual values at the bottom and top surfaces of layer k, respectively, and the interlaminar displacement continuity can be easily imposed as $\mathbf{u}_t^k = \mathbf{u}_b^{k+1}$. Following the nomenclature suggested by Carrera [21], each member of this family is here denoted by the acronym LDN, which stands for (L)ayerwise (D)isplacement-based theory of order N. Note that the number of degrees of freedom for a LDN theory depends on the number of layers of the laminated panel and is given by $3(N + 1)N_\ell - 3(N_\ell - 1)$.

The class of ESL theories considered here involves global thickness function as increasing power of the global thickness coordinate z, which is measured from the middle surface of the curved panel. Since the kinematics is layer-independent, the k index in Eq. (9) is dropped. Accordingly, $t = 0$, $b = 1$, and

$$
\begin{aligned}
F_0 &= 1 \\
F_1 &= z \\
F_r &= z^r \qquad (r = 2, \ldots, N)
\end{aligned}
\tag{12}
$$

The related N-order member of the ESL family is indicated by EDN, which stands for (E)quivalent single-layer (D)isplacement-based theory of order N.

Using Eq. (9), the geometric relations and constitutive equations of each layer of the curved panel are written, respectively, as

$$\boldsymbol{\varepsilon}_p^k = \left(\mathcal{D}_p^k + \mathcal{A}_p^k \right) F_\tau \mathbf{u}_\tau^k \qquad \boldsymbol{\varepsilon}_n^k = \left(\mathcal{D}_n^k - \mathcal{A}_n^k + \mathcal{D}_z^k \right) F_\tau \mathbf{u}_\tau^k \tag{13}$$

and

$$
\begin{aligned}
\boldsymbol{\sigma}_p^k &= \tilde{\mathbf{C}}_{pp}^k \left(\mathcal{D}_p^k + \mathcal{A}_p^k \right) F_s \mathbf{u}_s^k + \tilde{\mathbf{C}}_{pn}^k \left(\mathcal{D}_n^k - \mathcal{A}_n^k + \mathcal{D}_z^k \right) F_s \mathbf{u}_s^k \\
\boldsymbol{\sigma}_n^k &= \tilde{\mathbf{C}}_{pn}^{k\mathrm{T}} \left(\mathcal{D}_p^k + \mathcal{A}_p^k \right) F_s \mathbf{u}_s^k + \tilde{\mathbf{C}}_{nn}^k \left(\mathcal{D}_n^k - \mathcal{A}_n^k + \mathcal{D}_z^k \right) F_s \mathbf{u}_s^k
\end{aligned}
\tag{14}
$$

where the index s for the thickness functions in Eq. (14) has the same role of the index τ.

The equations of motion are here derived from the principle of virtual displacements (PVD), which, in absence of any external body and surface force, can be expressed as follows

$$\sum_{k=1}^{N_\ell} \int_{\Omega_k} \int_{\mathcal{Z}_k} \delta \mathbf{u}^{k\mathrm{T}} \rho^k \frac{\partial^2 \mathbf{u}^k}{\partial t^2} H_\alpha^k H_\beta^k \, \mathrm{d}z \, \mathrm{d}\alpha \, \mathrm{d}\beta + \sum_{k=1}^{N_\ell} \int_{\Omega_k} \int_{\mathcal{Z}_k} \left[\delta \boldsymbol{\varepsilon}_p^{k\mathrm{T}} \boldsymbol{\sigma}_p^k + \delta \boldsymbol{\varepsilon}_n^{k\mathrm{T}} \boldsymbol{\sigma}_n^k \right] H_\alpha^k H_\beta^k \, \mathrm{d}z \, \mathrm{d}\alpha \, \mathrm{d}\beta = 0 \tag{15}$$

where $\mathcal{Z}_k$ is the layer domain in the thickness direction. Using Eq. (9) and the geometric relations of Eqs. (13) into the above PVD statement, the dynamic equilibrium is expressed in weak form by the following equation

$$\sum_{k=1}^{N_\ell} \int_{\Omega_k} \delta\mathbf{u}_\tau^{k\mathrm{T}} \rho^k J_{\alpha\beta}^{k\tau s} \frac{\partial^2 \mathbf{u}_s^k}{\partial t^2} \, \mathrm{d}\alpha \, \mathrm{d}\beta + \sum_{k=1}^{N_\ell} \int_{\Omega_k} \int_{\mathcal{Z}_k} \left[\left(\mathcal{D}_\mathrm{p}^k \delta\mathbf{u}_\tau^k\right)^{\mathrm{T}} \boldsymbol{\sigma}_\mathrm{p}^k F_\tau + \left(\mathcal{D}_\mathrm{n}^k \delta\mathbf{u}_\tau^k\right)^{\mathrm{T}} \boldsymbol{\sigma}_\mathrm{n}^k F_\tau \right] H_\alpha^k H_\beta^k \, \mathrm{d}z \, \mathrm{d}\alpha \, \mathrm{d}\beta$$

$$+ \sum_{k=1}^{N_\ell} \int_{\Omega_k} \int_{\mathcal{Z}_k} \left[\delta\mathbf{u}_\tau^{k\mathrm{T}} \mathcal{A}_\mathrm{p}^{k\mathrm{T}} \boldsymbol{\sigma}_\mathrm{p}^k F_\tau - \delta\mathbf{u}_\tau^{k\mathrm{T}} \mathcal{A}_\mathrm{n}^{k\mathrm{T}} \boldsymbol{\sigma}_\mathrm{n}^k F_\tau \right] H_\alpha^k H_\beta^k \, \mathrm{d}z \, \mathrm{d}\alpha \, \mathrm{d}\beta + \sum_{k=1}^{N_\ell} \int_{\Omega_k} \int_{\mathcal{Z}_k} \delta\mathbf{u}_\tau^{k\mathrm{T}} \mathcal{D}_z^{k\mathrm{T}} \boldsymbol{\sigma}_\mathrm{n}^k F_\tau H_\alpha^k H_\beta^k \, \mathrm{d}z \, \mathrm{d}\alpha \, \mathrm{d}\beta = 0 \tag{16}$$

where

$$J_{\alpha\beta}^{k\tau s} = \int_{\mathcal{Z}_k} F_\tau F_s H_\alpha^k H_\beta^k \, \mathrm{d}z \tag{17}$$

is a thickness integral over the kth layer involving the product of thickness functions F_τ and F_s.

After integrating by parts the second term in Eq. (16), using the constitutive relations (14), and exploiting the arbitrariness of the virtual variation of each kinematic variable $\delta\mathbf{u}_\tau^k$ over Ω_k, the following set of differential equations in compact indicial notation is obtained:

$$\mathcal{L}^{k\tau s} \mathbf{u}_s^k = \mathcal{M}^{k\tau s} \frac{\partial^2 \mathbf{u}_s^k}{\partial t^2} \tag{18}$$

where $\mathcal{L}^{k\tau s}$ and $\mathcal{M}^{k\tau s}$ are 3×3 matrices of differential operators expressed as

$$\mathcal{L}^{k\tau s} = \int_{\mathcal{Z}_k} \left\{ \left(-\mathcal{D}_\mathrm{p}^k + \mathcal{A}_\mathrm{p}^k\right)^{\mathrm{T}} \tilde{\mathbf{C}}_\mathrm{pp}^k \left(\mathcal{D}_\mathrm{p}^k + \mathcal{A}_\mathrm{p}^k\right) + \left(-\mathcal{D}_\mathrm{p}^k + \mathcal{A}_\mathrm{p}^k\right)^{\mathrm{T}} \tilde{\mathbf{C}}_\mathrm{pn}^k \left(\mathcal{D}_\mathrm{n}^k - \mathcal{A}_\mathrm{n}^k + \mathcal{D}_z^k\right) \right.$$

$$\left. + \left(-\mathcal{D}_\mathrm{n}^k - \mathcal{A}_\mathrm{n}^k + \mathcal{D}_z^k\right)^{\mathrm{T}} \tilde{\mathbf{C}}_\mathrm{pn}^{k\mathrm{T}} \left(\mathcal{D}_\mathrm{p}^k + \mathcal{A}_\mathrm{p}^k\right) + \left(-\mathcal{D}_\mathrm{n}^k - \mathcal{A}_\mathrm{n}^k + \mathcal{D}_z^k\right)^{\mathrm{T}} \tilde{\mathbf{C}}_\mathrm{nn}^k \left(\mathcal{D}_\mathrm{n}^k - \mathcal{A}_\mathrm{n}^k + \mathcal{D}_z^k\right) \right\} F_\tau F_s H_\alpha^k H_\beta^k \, \mathrm{d}z \tag{19}$$

and

$$\mathcal{M}^{k\tau s} = \mathrm{diag}\left(\rho^k J_{\alpha\beta}^{k\tau s}\right) \tag{20}$$

It is noted that Eq. (18) is valid for any index τ and any layer k, and the summation for repeated index s is implied. Therefore, according to the order of the assumed shell theory and the number of layers of the curved panel, the expanded set of governing equations can be derived from Eq. (18) for each specific case under investigation. However, this set is not written in explicit form, since, according to Carrera's formulation, $\mathcal{L}^{k\tau s}$ and $\mathcal{M}^{k\tau s}$ are profitably viewed as invariant entities, which are directly expanded and assembled to build in a hierarchical and automatic manner the discretized stiffness and mass matrices of the free vibration problem, as explained later. For this reason, $\mathcal{L}^{k\tau s}$ and $\mathcal{M}^{k\tau s}$ are called the *fundamental nuclei* of the formulation [21].

Similarly, the arbitrariness of the virtual variation $\delta\mathbf{u}_\tau^k$ over the boundary of the panel yields the following set of boundary conditions

$$\mathcal{B}^{k\tau s} \mathbf{u}_s^k = \mathbf{0} \tag{21}$$

where $\mathcal{B}^{k\tau s}$ is another invariant 3×3 matrix of differential operators called fundamental nucleus related to the boundary conditions. It is given for Neumann-type boundary conditions by

$$\mathcal{B}^{k\tau s} = \int_{\mathcal{Z}_k} \left\{ \mathcal{N}_\mathrm{p}^{k\mathrm{T}} \tilde{\mathbf{C}}_\mathrm{pp}^k \left(\mathcal{D}_\mathrm{p}^k + \mathcal{A}_\mathrm{p}^k\right) + \mathcal{N}_\mathrm{p}^{k\mathrm{T}} \tilde{\mathbf{C}}_\mathrm{pn}^k \left(\mathcal{D}_\mathrm{n}^k - \mathcal{A}_\mathrm{n}^k + \mathcal{D}_z^k\right) + \mathcal{N}_\mathrm{n}^{k\mathrm{T}} \tilde{\mathbf{C}}_\mathrm{pn}^{k\mathrm{T}} \left(\mathcal{D}_\mathrm{p}^k + \mathcal{A}_\mathrm{p}^k\right) \right.$$

$$\left. + \mathcal{N}_\mathrm{n}^{k\mathrm{T}} \tilde{\mathbf{C}}_\mathrm{nn}^k \left(\mathcal{D}_\mathrm{n}^k - \mathcal{A}_\mathrm{n}^k + \mathcal{D}_z^k\right) \right\} F_\tau F_s H_\alpha^k H_\beta^k \, \mathrm{d}z \tag{22}$$

where $\mathcal{N}_\mathrm{p}^k$ and $\mathcal{N}_\mathrm{n}^k$ are matrices containing the components n_α and n_β of the unit normal vector to the boundary as follows

$$\mathcal{N}_\mathrm{p}^k = \begin{bmatrix} \frac{n_\alpha}{H_\alpha^k} & 0 & 0 \\ 0 & \frac{n_\beta}{H_\beta^k} & 0 \\ \frac{n_\beta}{H_\beta^k} & \frac{n_\alpha}{H_\alpha^k} & 0 \end{bmatrix} \qquad \mathcal{N}_\mathrm{n}^k = \begin{bmatrix} 0 & 0 & \frac{n_\alpha}{H_\alpha^k} \\ 0 & 0 & \frac{n_\beta}{H_\beta^k} \\ 0 & 0 & 0 \end{bmatrix} \tag{23}$$

Since we are interested in the computation of the natural frequencies of the panel, a harmonic solution $\mathbf{u}_s^k = \hat{\mathbf{u}}_s^k e^{j\omega t}$ is assumed. The corresponding differential eigenvalue problem is expressed by the equations

$$\mathcal{L}^{k\tau s}\hat{\mathbf{u}}_s^k = -\omega^2 \mathcal{M}^{k\tau s}\hat{\mathbf{u}}_s^k \tag{24}$$

and

$$\mathcal{B}^{k\tau s}\hat{\mathbf{u}}_s^k = \mathbf{0} \tag{25}$$

3 Spectral collocation solution

A spectral collocation solution of the eigenvalue problem described by Eqs. (24) and (25) is sought. First, a grid of Chebyshev-Gauss-Lobatto (CGL) points (α_i, β_j), $i, j = 0, \ldots, N_{\text{CGL}}$, over Ω_k is introduced [23]. The discrete solution of the problem is assumed in the form of tensor product of one-dimensional expansions as follows

$$\left\{ \begin{array}{c} \hat{u}_{\alpha s}^k \\ \hat{u}_{\beta s}^k \\ \hat{u}_{zs}^k \end{array} \right\} = \sum_{m=0}^{N_{\text{CGL}}} \sum_{n=0}^{N_{\text{CGL}}} \left\{ \begin{array}{c} \hat{u}_{\alpha smn}^k \\ \hat{u}_{\beta smn}^k \\ \hat{u}_{zsmn}^k \end{array} \right\} \psi_m(\alpha)\psi_n(\beta) \tag{26}$$

where $\hat{u}_{\alpha smn}^k$, $\hat{u}_{\beta smn}^k$ and $\hat{u}_{zsmn}^k$ are the unknown values of the kinematic quantities at the grid points, i.e., $\hat{u}_{\alpha smn}^k = \hat{u}_{\alpha s}^k(\alpha_m, \beta_n)$, $\hat{u}_{\beta smn}^k = \hat{u}_{\beta s}^k(\alpha_m, \beta_n)$ and $\hat{u}_{zsmn}^k = \hat{u}_{zs}^k(\alpha_m, \beta_n)$, and ψ_l ($l = 0, \ldots, N_{\text{CGL}}$) denotes the Lagrange interpolating polynomial relative to the given set of CGL nodes, so that $\psi_m(\alpha_i) = \delta_{mi}$ and $\psi_n(\beta_j) = \delta_{nj}$ for $i, j = 0, \ldots, N$. The approximation $(\hat{u}_{\alpha s}^k, \hat{u}_{\beta s}^k, \hat{u}_{zs}^k)$ is found by collocation; that is, $(\hat{u}_{\alpha s}^k, \hat{u}_{\beta s}^k, \hat{u}_{zs}^k)$ is required to satisfy the differential problem Eq. (24) along with the boundary conditions Eq. (25) at the CGL nodes. The derivatives in the differential operators $\mathcal{L}^{k\tau s}$ and $\mathcal{B}^{k\tau s}$ are approximated through the interpolation derivatives, corresponding to the evaluation at the grid points of the first- and second-order derivatives of the interpolants in Eq. (26) as shown below.

In order to simplify the writing and the coding process, the collocation equations are written in a matrix form. To this aim, the vectors $\mathbf{U}_{\alpha s}^k, \mathbf{U}_{\beta s}^k, \mathbf{U}_{zs}^k \in \mathbb{R}^{(N_{\text{CGL}}+1)^2}$ of values $\hat{u}_{\alpha smn}^k$, $\hat{u}_{\beta smn}^k$ and $\hat{u}_{zsmn}^k$ of the kinematic quantities at the CGL nodes are introduced as follows

$$\mathbf{U}_{\alpha s}^k = \left\{ \begin{array}{cccccc} \hat{u}_{\alpha s00} & \hat{u}_{\alpha s01} & \cdots & \hat{u}_{\alpha s0N_{\text{CGL}}} & \cdots & \hat{u}_{\alpha sN_{\text{CGL}}N_{\text{CGL}}} \end{array} \right\}^{\text{T}}$$

$$\mathbf{U}_{\beta s}^k = \left\{ \begin{array}{cccccc} \hat{u}_{\beta s00} & \hat{u}_{\beta s01} & \cdots & \hat{u}_{\beta s0N_{\text{CGL}}} & \cdots & \hat{u}_{\beta sN_{\text{CGL}}N_{\text{CGL}}} \end{array} \right\}^{\text{T}} \tag{27}$$

$$\mathbf{U}_{zs}^k = \left\{ \begin{array}{cccccc} \hat{u}_{zs00} & \hat{u}_{zs01} & \cdots & \hat{u}_{zs0N_{\text{CGL}}} & \cdots & \hat{u}_{zsN_{\text{CGL}}N_{\text{CGL}}} \end{array} \right\}^{\text{T}}$$

They are sorted so that increasing values of the coordinate α (β) of the curved panel correspond to increasing values of the index i (j). The values of the derivatives at the CGL points are also collected into vectors and are expressed in terms of the quantities in Eq. (27) by using the differentiation matrices $\mathbf{D}_1$ and $\mathbf{D}_2$ which contain the first- and second-order derivatives, respectively, of the interpolants evaluated at the CGL nodes [30]. We have $\mathbf{D}_2 = \mathbf{D}_1^2$ and the entries of $\mathbf{D}_1$ are reported in [30]. For example, the evaluation of $\partial \hat{u}_{\alpha s}^k / \partial \alpha$ at the collocation points is expressed as $(\mathbf{D}_1 \otimes \mathbf{I})\mathbf{U}_{\alpha s}^k$, where $\mathbf{I}$ is the $(N_{\text{CGL}} + 1) \times (N_{\text{CGL}} + 1)$ identity matrix and $\otimes$ is the Kronecker product. Similarly, $\partial^2 \hat{u}_{zs}^k / \partial \beta^2$ evaluated at the CGL nodes is given by $(\mathbf{I} \otimes \mathbf{D}_2)\mathbf{U}_{zs}^k$, and so on.

By using the above notation, the following collocated equations expressed in the same indicial and invariant form of the original differential equations are obtained

$$\begin{bmatrix} \mathbf{K}_{11}^{k\tau s} & \mathbf{K}_{12}^{k\tau s} & \mathbf{K}_{13}^{k\tau s} \\ \mathbf{K}_{21}^{k\tau s} & \mathbf{K}_{22}^{k\tau s} & \mathbf{K}_{23}^{k\tau s} \\ \mathbf{K}_{31}^{k\tau s} & \mathbf{K}_{32}^{k\tau s} & \mathbf{K}_{33}^{k\tau s} \end{bmatrix} \left\{ \begin{array}{c} \mathbf{U}_{\alpha s}^k \\ \mathbf{U}_{\beta s}^k \\ \mathbf{U}_{zs}^k \end{array} \right\} = \omega^2 \begin{bmatrix} \mathbf{M}_{11}^{k\tau s} & \mathbf{0} & \mathbf{0} \\ \mathbf{0} & \mathbf{M}_{22}^{k\tau s} & \mathbf{0} \\ \mathbf{0} & \mathbf{0} & \mathbf{M}_{33}^{k\tau s} \end{bmatrix} \left\{ \begin{array}{c} \mathbf{U}_{\alpha s}^k \\ \mathbf{U}_{\beta s}^k \\ \mathbf{U}_{zs}^k \end{array} \right\} \tag{28}$$

or, more compactly,

$$\mathbf{K}^{k\tau s}\mathbf{U}_s^k = \omega^2 \mathbf{M}^{k\tau s}\mathbf{U}_s^k \tag{29}$$

where

$$\mathbf{K}_{11}^{k\tau s} = \tilde{C}_{55}^{k}\left(J_{\alpha\beta}^{k\tau_z s_z} + \frac{1}{R_\alpha^{k\,2}}J_{\beta/\alpha}^{k\tau s} - \frac{1}{R_\alpha^{k}}J_{\beta}^{k\tau_z s} - \frac{1}{R_\alpha^{k}}J_{\beta}^{k\tau s_z}\right)(\mathbf{I}\otimes\mathbf{I}) - \tilde{C}_{11}^{k}J_{\beta/\alpha}^{k\tau s}(\mathbf{D}_2\otimes\mathbf{I}) - 2\tilde{C}_{16}^{k}J^{k\tau s}(\mathbf{D}_1\otimes\mathbf{D}_1) - \tilde{C}_{66}^{k}J_{\alpha/\beta}^{k\tau s}(\mathbf{I}\otimes\mathbf{D}_2)$$

$$\mathbf{K}_{12}^{k\tau s} = \tilde{C}_{45}^{k}\left(J_{\alpha\beta}^{k\tau_z s_z} + \frac{1}{R_\alpha^{k}R_\beta^{k}}J^{k\tau s} - \frac{1}{R_\alpha^{k}}J_{\beta}^{k\tau s_z} - \frac{1}{R_\beta^{k}}J_{\alpha}^{k\tau_z s}\right)(\mathbf{I}\otimes\mathbf{I}) - (\tilde{C}_{12}^{k}+\tilde{C}_{66}^{k})J^{k\tau s}(\mathbf{D}_1\otimes\mathbf{D}_1) - \tilde{C}_{16}^{k}J_{\beta/\alpha}^{k\tau s}(\mathbf{D}_2\otimes\mathbf{I}) - \tilde{C}_{26}^{k}J_{\alpha/\beta}^{k\tau s}(\mathbf{I}\otimes\mathbf{D}_2)$$

$$\mathbf{K}_{13}^{k\tau s} = \left[\tilde{C}_{55}^{k}\left(J_{\beta}^{k\tau_z s} - \frac{1}{R_\alpha^{k}}J_{\beta/\alpha}^{k\tau s}\right) - \tilde{C}_{11}^{k}\frac{1}{R_\alpha^{k}}J_{\beta/\alpha}^{k\tau s} - \tilde{C}_{12}^{k}\frac{1}{R_\beta^{k}}J^{k\tau s} - \tilde{C}_{13}^{k}J_{\beta}^{k\tau s_z}\right](\mathbf{D}_1\otimes\mathbf{I}) + \left[\tilde{C}_{45}^{k}\left(J_{\alpha}^{k\tau_z s} - \frac{1}{R_\alpha^{k}}J^{k\tau s}\right) - \tilde{C}_{16}^{k}\frac{1}{R_\alpha^{k}}J^{k\tau s}\right.$$
$$\left. - \tilde{C}_{26}^{k}\frac{1}{R_\beta^{k}}J_{\alpha/\beta}^{k\tau s} - \tilde{C}_{36}^{k}J_{\alpha}^{k\tau s_z}\right](\mathbf{I}\otimes\mathbf{D}_1)$$

$$\mathbf{K}_{21}^{k\tau s} = \tilde{C}_{45}^{k}\left(J_{\alpha\beta}^{k\tau_z s_z} + \frac{1}{R_\alpha^{k}R_\beta^{k}}J^{k\tau s} - \frac{1}{R_\alpha^{k}}J_{\beta}^{k\tau_z s} - \frac{1}{R_\beta^{k}}J_{\alpha}^{k\tau s_z}\right)(\mathbf{I}\otimes\mathbf{I}) - (\tilde{C}_{12}^{k}+\tilde{C}_{66}^{k})J^{k\tau s}(\mathbf{D}_1\otimes\mathbf{D}_1) - \tilde{C}_{16}^{k}J_{\beta/\alpha}^{k\tau s}(\mathbf{D}_2\otimes\mathbf{I}) - \tilde{C}_{26}^{k}J_{\alpha/\beta}^{k\tau s}(\mathbf{I}\otimes\mathbf{D}_2)$$

$$\mathbf{K}_{22}^{k\tau s} = \tilde{C}_{44}^{k}\left(J_{\alpha\beta}^{k\tau_z s_z} + \frac{1}{R_\beta^{k\,2}}J_{\alpha/\beta}^{k\tau s} - \frac{1}{R_\beta^{k}}J_{\alpha}^{k\tau_z s} - \frac{1}{R_\beta^{k}}J_{\alpha}^{k\tau s_z}\right)(\mathbf{I}\otimes\mathbf{I}) - \tilde{C}_{22}^{k}J_{\alpha/\beta}^{k\tau s}(\mathbf{I}\otimes\mathbf{D}_2) - 2\tilde{C}_{26}^{k}J^{k\tau s}(\mathbf{D}_1\otimes\mathbf{D}_1) - \tilde{C}_{66}^{k}J_{\beta/\alpha}^{k\tau s}(\mathbf{D}_2\otimes\mathbf{I})$$

$$\mathbf{K}_{23}^{k\tau s} = \left[\tilde{C}_{45}^{k}\left(J_{\beta}^{k\tau_z s} - \frac{1}{R_\beta^{k}}J^{k\tau s}\right) - \tilde{C}_{16}^{k}\frac{1}{R_\alpha^{k}}J_{\beta/\alpha}^{k\tau s} - \tilde{C}_{26}^{k}\frac{1}{R_\beta^{k}}J^{k\tau s} - \tilde{C}_{36}^{k}J_{\beta}^{k\tau s_z}\right](\mathbf{D}_1\otimes\mathbf{I}) + \left[\tilde{C}_{44}^{k}\left(J_{\alpha}^{k\tau_z s} - \frac{1}{R_\beta^{k}}J_{\alpha/\beta}^{k\tau s}\right) - \tilde{C}_{12}^{k}\frac{1}{R_\alpha^{k}}J^{k\tau s}\right.$$
$$\left. - \tilde{C}_{22}^{k}\frac{1}{R_\beta^{k}}J_{\alpha/\beta}^{k\tau s} - \tilde{C}_{23}^{k}J_{\alpha}^{k\tau s_z}\right](\mathbf{I}\otimes\mathbf{D}_1)$$

$$\mathbf{K}_{31}^{k\tau s} = \left[\tilde{C}_{11}^{k}\frac{1}{R_\alpha^{k}}J_{\beta/\alpha}^{k\tau s} + \tilde{C}_{12}^{k}\frac{1}{R_\beta^{k}}J^{k\tau s} + \tilde{C}_{55}^{k}\left(\frac{1}{R_\alpha^{k}}J_{\beta/\alpha}^{k\tau s} - J_{\beta}^{k\tau s_z}\right) + \tilde{C}_{13}^{k}J_{\beta}^{k\tau_z s}\right](\mathbf{D}_1\otimes\mathbf{I}) + \left[\tilde{C}_{16}^{k}\frac{1}{R_\alpha^{k}}J^{k\tau s} + \tilde{C}_{26}^{k}\frac{1}{R_\beta^{k}}J_{\alpha/\beta}^{k\tau s} + \tilde{C}_{36}^{k}J_{\alpha}^{k\tau_z s}\right.$$
$$\left. + \tilde{C}_{45}^{k}\left(\frac{1}{R_\alpha^{k}}J^{k\tau s} - J_{\alpha}^{k\tau s_z}\right)\right](\mathbf{I}\otimes\mathbf{D}_1)$$

$$\mathbf{K}_{32}^{k\tau s} = \left[\frac{\tilde{C}_{16}^{k}}{R_\alpha^{k}}J_{\beta/\alpha}^{k\tau s} + \frac{\tilde{C}_{26}^{k}}{R_\beta^{k}}J^{k\tau s} + \tilde{C}_{45}^{k}\left(\frac{1}{R_\beta^{k}}J^{k\tau s} - J_{\beta}^{k\tau s_z}\right) + \tilde{C}_{36}^{k}J_{\beta}^{k\tau_z s}\right](\mathbf{D}_1\otimes\mathbf{I}) + \left[\frac{\tilde{C}_{12}^{k}}{R_\alpha^{k}}J^{k\tau s} + \frac{\tilde{C}_{22}^{k}}{R_\beta^{k}}J_{\alpha/\beta}^{k\tau s} + \tilde{C}_{23}^{k}J_{\alpha}^{k\tau_z s}\right.$$
$$\left. + \tilde{C}_{44}^{k}\left(\frac{1}{R_\beta^{k}}J_{\alpha/\beta}^{k\tau s} - J_{\alpha}^{k\tau s_z}\right)\right](\mathbf{I}\otimes\mathbf{D}_1)$$

$$\mathbf{K}_{33}^{k\tau s} = \left[\tilde{C}_{33}^{k}J_{\alpha\beta}^{k\tau_z s_z} + \frac{1}{R_\alpha^{k}}\left(\frac{\tilde{C}_{11}^{k}}{R_\alpha^{k}}J_{\beta/\alpha}^{k\tau s} + 2\frac{\tilde{C}_{12}^{k}}{R_\beta^{k}}J^{k\tau s} + \tilde{C}_{13}^{k}J_{\beta}^{k\tau s_z} + \tilde{C}_{13}^{k}J_{\beta}^{k\tau_z s}\right) + \frac{1}{R_\beta^{k}}\left(\tilde{C}_{22}^{k}\frac{1}{R_\beta^{k}}J_{\alpha/\beta}^{k\tau s} + \tilde{C}_{23}^{k}J_{\alpha}^{k\tau s_z} + \tilde{C}_{23}^{k}J_{\alpha}^{k\tau_z s}\right)\right](\mathbf{I}\otimes\mathbf{I})$$
$$ - \tilde{C}_{55}^{k}J_{\beta/\alpha}^{k\tau s}(\mathbf{D}_2\otimes\mathbf{I}) - 2\tilde{C}_{45}^{k}J^{k\tau s}(\mathbf{D}_1\otimes\mathbf{D}_1) - \tilde{C}_{44}^{k}J_{\alpha/\beta}^{k\tau s}(\mathbf{I}\otimes\mathbf{D}_2)$$

are the $(N_{CGL}+1)^2 \times (N_{CGL}+1)^2$ element matrices of the discrete stiffness-related fundamental nucleus $\mathbf{K}^{k\tau s}$ arising from the spectral collocation process, and

$$\mathbf{M}_{11}^{k\tau s} = \rho^{k}J_{\alpha\beta}^{k\tau s}(\mathbf{I}\otimes\mathbf{I})$$

$$\mathbf{M}_{22}^{k\tau s} = \rho^{k}J_{\alpha\beta}^{k\tau s}(\mathbf{I}\otimes\mathbf{I})$$

$$\mathbf{M}_{33}^{k\tau s} = \rho^{k}J_{\alpha\beta}^{k\tau s}(\mathbf{I}\otimes\mathbf{I})$$

are the $(N_{CGL}+1)^2 \times (N_{CGL}+1)^2$ element matrices of the discrete mass-related fundamental nucleus $\mathbf{M}^{k\tau s}$. In the above nuclei, $J^{k\tau s}, J_{\alpha}^{k\tau s}, \dots$ are thickness integrals defined in Appendix.

Similarly, the discretization of the boundary conditions yields

$$\begin{bmatrix} \mathbf{B}_{11}^{k\tau s} & \mathbf{B}_{12}^{k\tau s} & \mathbf{B}_{13}^{k\tau s} \\ \mathbf{B}_{21}^{k\tau s} & \mathbf{B}_{22}^{k\tau s} & \mathbf{B}_{23}^{k\tau s} \\ \mathbf{B}_{31}^{k\tau s} & \mathbf{B}_{32}^{k\tau s} & \mathbf{B}_{33}^{k\tau s} \end{bmatrix} \begin{Bmatrix} \mathbf{U}_{\alpha s}^{k} \\ \mathbf{U}_{\beta s}^{k} \\ \mathbf{U}_{zs}^{k} \end{Bmatrix} = \mathbf{0} \tag{30}$$

or, more compactly,

$$\mathbf{B}^{k\tau s}\mathbf{U}_s^k = \mathbf{0} \tag{31}$$

The element matrices $\mathbf{B}_{ij}^{k\tau s}$ of the discrete fundamental nucleus $\mathbf{B}^{k\tau s}$ related to Neumann-type boundary conditions are given by

$$\mathbf{B}_{11}^{k\tau s} = n_\alpha \left[\tilde{C}_{11}^k J_{\beta/\alpha}^{k\tau s} \left(\mathbf{e}_b^{\mathrm{T}} \mathbf{D}_1 \otimes \mathbf{I} \right) + \tilde{C}_{16}^k J^{k\tau s} \left(\mathbf{e}_b^{\mathrm{T}} \otimes \mathbf{D}_1 \right) \right] + n_\beta \left[\tilde{C}_{16}^k J^{k\tau s} \left(\mathbf{D}_1 \otimes \mathbf{e}_b^{\mathrm{T}} \right) + \tilde{C}_{66}^k J_{\alpha/\beta}^{k\tau s} \left(\mathbf{I} \otimes \mathbf{e}_b^{\mathrm{T}} \mathbf{D}_1 \right) \right]$$

$$\mathbf{B}_{12}^{k\tau s} = n_\alpha \left[\tilde{C}_{16}^k J_{\beta/\alpha}^{k\tau s} \left(\mathbf{e}_b^{\mathrm{T}} \mathbf{D}_1 \otimes \mathbf{I} \right) + \tilde{C}_{12}^k J^{k\tau s} \left(\mathbf{e}_b^{\mathrm{T}} \otimes \mathbf{D}_1 \right) \right] + n_\beta \left[\tilde{C}_{66}^k J^{k\tau s} \left(\mathbf{D}_1 \otimes \mathbf{e}_b^{\mathrm{T}} \right) + \tilde{C}_{26}^k J_{\alpha/\beta}^{k\tau s} \left(\mathbf{I} \otimes \mathbf{e}_b^{\mathrm{T}} \mathbf{D}_1 \right) \right]$$

$$\mathbf{B}_{13}^{k\tau s} = n_\alpha \left[\frac{1}{R_\alpha^k} \tilde{C}_{11}^k J_{\beta/\alpha}^{k\tau s} + \frac{1}{R_\beta^k} \tilde{C}_{12}^k J^{k\tau s} + \tilde{C}_{13}^k J_\beta^{k\tau s_z} \right] \left(\mathbf{e}_b^{\mathrm{T}} \otimes \mathbf{I} \right) + n_\beta \left[\frac{1}{R_\alpha^k} \tilde{C}_{16}^k J^{k\tau s} + \frac{1}{R_\beta^k} \tilde{C}_{26}^k J_{\alpha/\beta}^{k\tau s} + \tilde{C}_{36}^k J_\alpha^{k\tau s_z} \right] \left(\mathbf{I} \otimes \mathbf{e}_b^{\mathrm{T}} \right)$$

$$\mathbf{B}_{21}^{k\tau s} = n_\alpha \left[\tilde{C}_{16}^k J_{\beta/\alpha}^{k\tau s} \left(\mathbf{e}_b^{\mathrm{T}} \mathbf{D}_1 \otimes \mathbf{I} \right) + \tilde{C}_{66}^k J^{k\tau s} \left(\mathbf{e}_b^{\mathrm{T}} \otimes \mathbf{D}_1 \right) \right] + n_\beta \left[\tilde{C}_{12}^k J^{k\tau s} \left(\mathbf{D}_1 \otimes \mathbf{e}_b^{\mathrm{T}} \right) + \tilde{C}_{26}^k J_{\alpha/\beta}^{k\tau s} \left(\mathbf{I} \otimes \mathbf{e}_b^{\mathrm{T}} \mathbf{D}_1 \right) \right]$$

$$\mathbf{B}_{22}^{k\tau s} = n_\alpha \left[\tilde{C}_{66}^k J_{\beta/\alpha}^{k\tau s} \left(\mathbf{e}_b^{\mathrm{T}} \mathbf{D}_1 \otimes \mathbf{I} \right) + \tilde{C}_{26}^k J^{k\tau s} \left(\mathbf{e}_b^{\mathrm{T}} \otimes \mathbf{D}_1 \right) \right] + n_\beta \left[\tilde{C}_{26}^k J^{k\tau s} \left(\mathbf{D}_1 \otimes \mathbf{e}_b^{\mathrm{T}} \right) + \tilde{C}_{22}^k J_{\alpha/\beta}^{k\tau s} \left(\mathbf{I} \otimes \mathbf{e}_b^{\mathrm{T}} \mathbf{D}_1 \right) \right]$$

$$\mathbf{B}_{23}^{k\tau s} = n_\alpha \left[\frac{1}{R_\alpha^k} \tilde{C}_{16}^k J_{\beta/\alpha}^{k\tau s} + \frac{1}{R_\beta^k} \tilde{C}_{26}^k J^{k\tau s} + \tilde{C}_{36}^k J_\beta^{k\tau s_z} \right] \left(\mathbf{e}_b^{\mathrm{T}} \otimes \mathbf{I} \right) + n_\beta \left[\frac{1}{R_\alpha^k} \tilde{C}_{12}^k J^{k\tau s} + \frac{1}{R_\beta^k} \tilde{C}_{22}^k J_{\alpha/\beta}^{k\tau s} + \tilde{C}_{23}^k J_\alpha^{k\tau s_z} \right] \left(\mathbf{I} \otimes \mathbf{e}_b^{\mathrm{T}} \right)$$

$$\mathbf{B}_{31}^{k\tau s} = n_\alpha \left[\tilde{C}_{55}^k J_\beta^{k\tau s_z} - \frac{1}{R_\alpha^k} \tilde{C}_{55}^k J_{\beta/\alpha}^{k\tau s} \right] \left(\mathbf{e}_b^{\mathrm{T}} \otimes \mathbf{I} \right) + n_\beta \left[\tilde{C}_{45}^k J_\alpha^{k\tau s_z} - \frac{1}{R_\alpha^k} \tilde{C}_{45}^k J^{k\tau s} \right] \left(\mathbf{I} \otimes \mathbf{e}_b^{\mathrm{T}} \right)$$

$$\mathbf{B}_{32}^{k\tau s} = n_\alpha \left[\tilde{C}_{45}^k J_\beta^{k\tau s_z} - \frac{1}{R_\beta^k} \tilde{C}_{45}^k J^{k\tau s} \right] \left(\mathbf{e}_b^{\mathrm{T}} \otimes \mathbf{I} \right) + n_\beta \left[\tilde{C}_{44}^k J_\alpha^{k\tau s_z} - \frac{1}{R_\beta^k} \tilde{C}_{44}^k J_{\alpha/\beta}^{k\tau s} \right] \left(\mathbf{I} \otimes \mathbf{e}_b^{\mathrm{T}} \right)$$

$$\mathbf{B}_{33}^{k\tau s} = n_\alpha \left[\tilde{C}_{55}^k J_{\beta/\alpha}^{k\tau s} \left(\mathbf{e}_b^{\mathrm{T}} \mathbf{D}_1 \otimes \mathbf{I} \right) + \tilde{C}_{45}^k J^{k\tau s} \left(\mathbf{e}_b^{\mathrm{T}} \otimes \mathbf{D}_1 \right) \right] + n_\beta \left[\tilde{C}_{45}^k J^{k\tau s} \left(\mathbf{D}_1 \otimes \mathbf{e}_b^{\mathrm{T}} \right) + \tilde{C}_{44}^k J_{\alpha/\beta}^{k\tau s} \left(\mathbf{I} \otimes \mathbf{e}_b^{\mathrm{T}} \mathbf{D}_1 \right) \right]$$

where $\mathbf{e}_b$ is a $(N_{\mathrm{CGL}} + 1)^2$ boundary unit vector, i.e., a vector having all elements equal to zero except for one element equal to one corresponding to the panel edge under consideration.
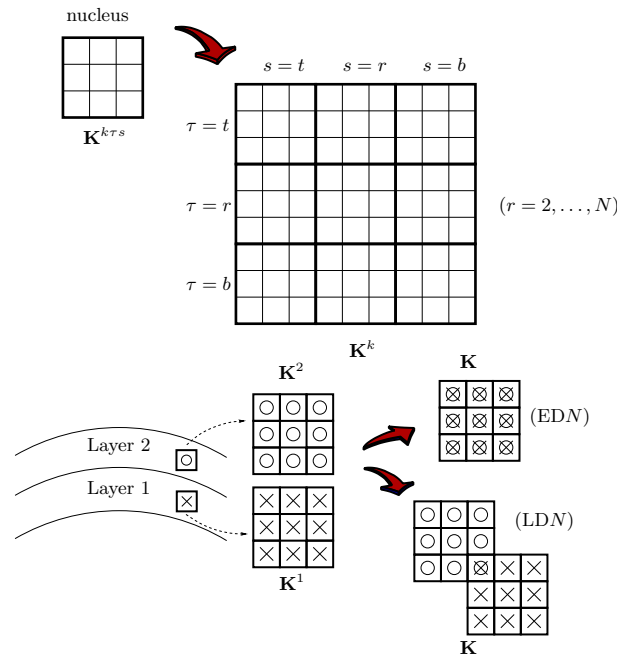
Figure 2: Graphical representation of the expansion and assembly procedure to transform the discrete fundamental nuclei of the formulation into the final discrete matrices governing the problem. Example of a curved panel with two layers.

As outlined before, the final set of discretized equations involving the global stiffness and mass matrices of the panel and the final set of related boundary conditions are obtained directly from the discrete fundamental nuclei $\mathbf{K}^{k\tau s}$, $\mathbf{M}^{k\tau s}$ and $\mathbf{B}^{k\tau s}$ by a simple expansion and assembly-like procedure, which is graphically represented in Figure 2 for the stiffness nucleus $\mathbf{K}^{k\tau s}$. The same procedure is applied to the mass $\mathbf{M}^{k\tau s}$ and the boundary $\mathbf{B}^{k\tau s}$ nuclei. First, the discrete nuclei are expanded by varying the theory-related indices τ and s to yield

$$\mathbf{K}^k \mathbf{U}^k = \omega^2 \mathbf{M}^k \mathbf{U}^k \qquad (32)$$

and

$$\mathbf{B}^k \mathbf{U}^k = \mathbf{0} \qquad (33)$$

where

$$\mathbf{U}^k = \left\{ \begin{array}{c} \mathbf{U}_t^k \\ \mathbf{U}_r^k \\ \mathbf{U}_b^k \end{array} \right\} \qquad (34)$$

$$\mathbf{K}^k = \left[\begin{array}{ccc} \mathbf{K}^{ktt} & \mathbf{K}^{ktr} & \mathbf{K}^{ktb} \\ \mathbf{K}^{krt} & \mathbf{K}^{krr} & \mathbf{K}^{krb} \\ \mathbf{K}^{kbt} & \mathbf{K}^{kbr} & \mathbf{K}^{kbb} \end{array} \right] \qquad (35)$$

and $\mathbf{M}^k$ and $\mathbf{B}^k$ matrices are built in a similar way. Afterwards, the multilayered matrices are assembled by varying the index k. This yields

$$\mathbf{KU} = \omega^2 \mathbf{MU} \qquad (36)$$

and

$$\mathbf{BU} = \mathbf{0} \qquad (37)$$

where $\mathbf{K}$, $\mathbf{M}$ and $\mathbf{B}$ are simply summed layer-by-layer in the case of ESL theories, or they are assembled as shown in Figure 2 by enforcing the interlaminar continuity condition in the case of LW theories.

Since the equations of motion must be enforced at the interior CGL points only and the boundary points must be explicitly defined in order to connect the differential problem with the set of boundary conditions, the final step of the spectral collocation process implies that Eqs. (36) and (37) are rewritten by partitioning the vector of unknown degrees of freedom $\mathbf{U}$ and the related matrices into quantities related to domain interior points (I) and quantities related to boundary points (B). Therefore, the previous eigenvalue problem can be expressed as

$$\mathbf{K}_B \mathbf{U}_B + \mathbf{K}_I \mathbf{U}_I = \omega^2 \mathbf{M}_I \mathbf{U}_I \qquad (38)$$

$$\mathbf{B}_B \mathbf{U}_B + \mathbf{B}_I \mathbf{U}_I = \mathbf{0} \qquad (39)$$

From the second equation, we have

$$\mathbf{U}_B = -\mathbf{B}_B^{-1} \mathbf{B}_I \mathbf{U}_I \qquad (40)$$

Substituting Eq. (40) into Eq. (38), the natural frequencies of the curved panel can be obtained by solving the following generalized eigenvalue problem

$$\left(\mathbf{K}_I - \mathbf{K}_B \mathbf{B}_B^{-1} \mathbf{B}_I \right) \mathbf{U}_I = \omega^2 \mathbf{M}_I \mathbf{U}_I \qquad (41)$$

4 Numerical examples

This section presents some illustrative numerical examples with the aim of showing the convergence properties, versatility and accuracy of the modeling and solution framework proposed in this work. The curved panels have side lengths a and b in the α and β direction, respectively, as shown in Figure 1. In all examples, the boundary conditions of the panel are denoted by a four-letter notation numbered in a counterclockwise direction starting from edge $\alpha = 0$. Both single-layer and multilayered panels made of isotropic and orthotropic material are considered. The properties for orthotropic material are the following: $E_1/E_2 = 25$, $G_{12}/E_2 = G_{13}/E_2 = 0.5$, $G_{23}/E_2 = 0.2$, $\nu_{12} = \nu_{13} = \nu_{23} = 0.25$. The mass density is taken as a reference dimensionless value of $\rho = 1$. For laminated panels, the layers are assumed to have the same thickness h_k.
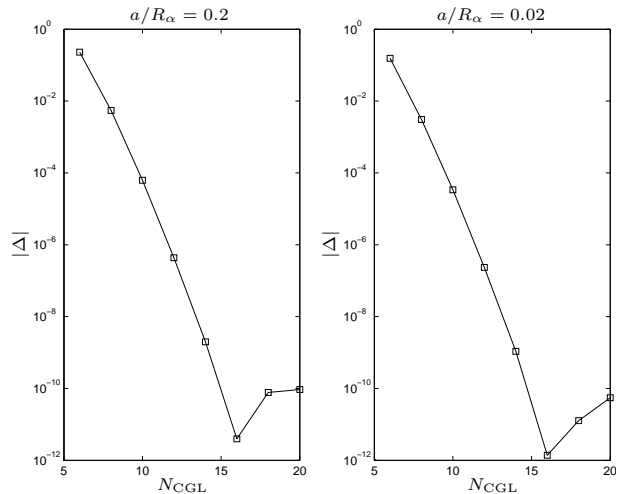
Figure 3: Convergence analysis. Fundamental frequency $\lambda = \omega(a^2/h)\sqrt{\rho/E_2}$ of a moderately thick ($a/h = 10$) square simply supported [0/90/0] spherical panel with $a/R_\alpha = 0.2$ and $a/R_\alpha = 0.02$. Values computed using ED2 theory.

The convergence rate of the spectral collocation solution is first examined in Figure 3, which reports the log plot of the absolute value of $\Delta = \lambda^{N_{CGL}} - \lambda^{N_{CGL}-2}$, where $\lambda_{N_{CGL}}$ denotes the fundamental non dimensional frequency parameter $\omega(a^2/h)\sqrt{\rho/E_2}$ computed using N_{CGL} colloca-

tion points along α and β direction. N_{CGL} is varied in the analysis from 6 to 20 with a step of 2. The computations are referred to a moderately thick ($a/h = 10$) square fully simply-supported (SSSS) spherical panel having [0/90/0] layup and two different shallowness ratios, $a/R_\alpha = 0.2$ (moderately deep panel) and $a/R_\alpha = 0.02$ (shallow panel). Values are obtained in both cases using the ED2 shell theory. It is shown that the spectral solutions exhibit a very fast convergence rate with an exponential decrease of Δ as the number of CGL points increases. The difference is so small for $N_{CGL} \geq 14$ that it is swamped by the round-off errors of the numerical computations.
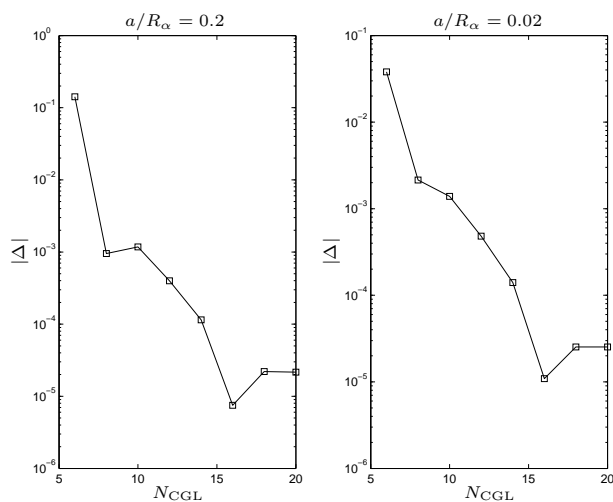
Figure 4: Convergence analysis. Fundamental frequency $\lambda = \omega(a^2/h)\sqrt{\rho/E_2}$ of a moderately thick ($a/h = 10$) square fully clamped [0/90/0] spherical panel with $a/R_\alpha = 0.2$ and $a/R_\alpha = 0.02$. Values computed using ED2 theory.

The same spherical panel of the previous case but with fully clamped (CCCC) edge conditions is considered in Figure 4. The fundamental frequency of the problem is again computed using ED2 theory. It is observed that the clamped boundaries largely affect the convergence properties of the solution. Although converged results to five significant digits are obtained using a relatively low number of collocation points, clamped edge conditions slow down the rate of convergence. Apparently, no further improvement of the approximate solution occurs when $N_{CGL} > 14$.

The adversing effect of clamped edges on the convergence properties of the present spectral solution is also found in other cases. For example, Figure 5 shows the difference between two successive approximations evaluated increasing by two the number of collocation points for the first four dimensionless frequencies $\lambda_i = \omega_i(a^2/h)\sqrt{\rho/E_2}$ of a moderately thick ($a/h = 10$) square fully clamped
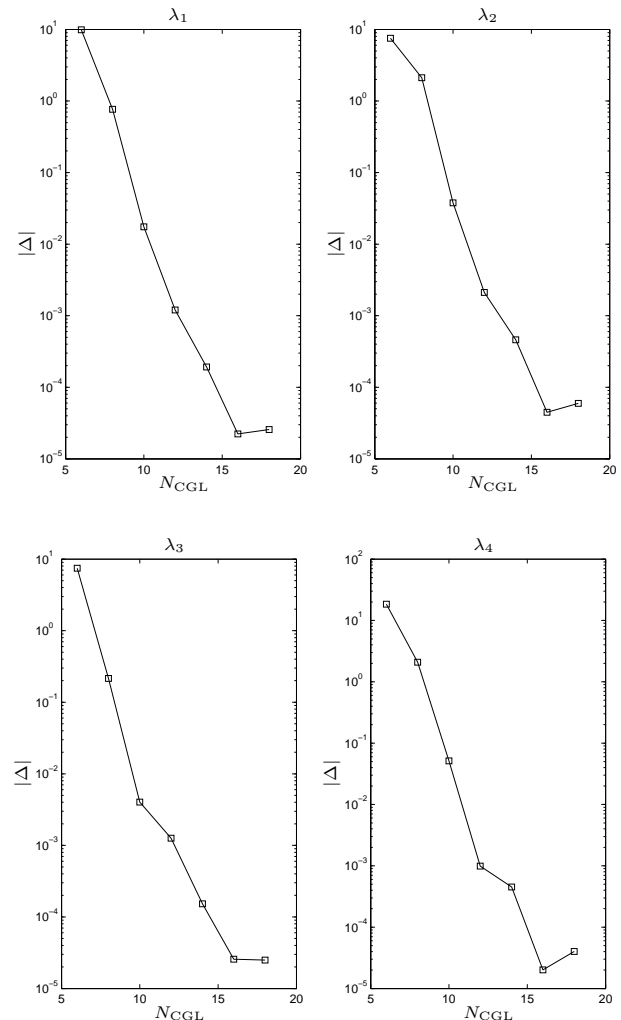
Figure 5: Convergence analysis. First four dimensionless frequencies $\lambda_i = \omega_i(a^2/h)\sqrt{\rho/E_2}$ of a moderately thick ($a/h = 10$) square fully clamped [45/ − 45]$_3$ deep cylindrical panel with $a/R_\beta = 2$. Values computed using LD1 theory.

[45/ − 45]$_3$ deep cylindrical panel with $a/R_\beta = 2$. In this case, N_{CGL} is varied from 6 to 18, and the results are obtained with a LD1 theory. It is noted that the convergence rate is similar to the case of a fully clamped spherical panel and is not significantly affected by the lamination lay-up, the shallowness ratio and the shell theory. Furthermore, no notable difference is observed as the number of mode to be estimated increases.

Similar trends of those shown in the previous figures have been observed in many other numerical cases, which are not presented here for the sake of brevity. It can be argued that sufficiently well converged values for the natural frequencies of the curved panels under study are obtained with $N_{CGL} = 14$, which is the number of collocation points used in the following comparison analysis.

Table 1: Non-dimensional frequency parameters $\lambda = \omega(a^2/h)\sqrt{\frac{\rho}{E}}$ of isotropic SSSS square cylindrical panels ($\nu = 0.25$).

a/h	a/R_β	Theory	λ_1	λ_2	λ_3	λ_4	λ_5
20	0.5	ED2	7.6166	14.650	16.587	23.574	28.664
		ED3	7.5523	14.423	16.390	23.206	28.183
		[15]	7.5523	14.423	16.390	23.206	28.183
	1	ED2	11.046	14.658	21.300	24.700	28.359
		ED3	11.017	14.444	21.166	24.369	27.885
		[15]	11.017	14.444	21.166	24.368	27.884
	2	ED2	14.725	17.905	27.179	28.544	33.468
		ED3	14.562	17.945	26.727	28.324	33.455
		[15]	14.562	17.945	26.727	28.324	33.455
10	0.5	ED2	6.1750	13.813	14.365	19.483	19.485
		ED3	6.0921	13.560	14.125	19.869	19.871
		[15]	6.0921	13.560	14.124	19.869	19.871
	1	ED2	7.1361	13.555	15.652	19.483	19.491
		ED3	7.0810	13.310	15.453	19.869	19.877
		[15]	7.0810	13.309	15.452	19.869	19.877
	2	ED2	9.5723	12.612	19.483	21.727	24.670
		ED3	9.5791	12.398	19.657	21.404	24.136
		[15]	9.5791	12.397	19.657	21.401	24.131

The accuracy of the modeling approach proposed in this paper is now evaluated and discussed by comparing the present solutions computed on models relying on shell theories of different topology and order with some reference solutions existing in the literature.

Two cases involving isotropic panels are first considered. One example deals with a SSSS square ($a = b$) cylindrical panel having two different span-to-thickness ratios $a/h = 20$ and $a/h = 10$ and three shallowness ratios $a/R_\beta = 0.5$, 1 and 2. Table 1 lists the first five natural frequency parameters $\lambda_i = \omega_i(a^2/h)\sqrt{\rho/E}$ found using the present approach with ED2 and ED3 theories. Results are compared against those obtained by [15] using 3-D elasticity from a high-fidelity finite element model. It can be seen that the third-order shear and normal deformation theory predicts all five frequencies very close to 3-D results. Values from ED2 models are quite accurate for the fundamental mode. However, the accuracy deteriorates as the vibration mode number increases. The second case of isotropic panels considered here involves CCCC square spherical shells with $a/R_\alpha = 0.5$ and length-to-thickness ratios $a/h = 10$ and $a/h = 5$. Non-dimensional frequency

parameters $\lambda_i = \omega_i a \sqrt{\frac{\rho}{E}}$ computed using a fourth-order ED4 theory are shown in Table 2 and compared with the 3-D elasticity solutions obtained by [14] from Ritz models. A good agreement is observed even when a thick panel is considered.

Fully clamped composite laminated cylindrical panels are examined in Tables 3 and 4. Both cases are referred to a square moderately thick deep panel with $a/h = 10$ and $a/R_\beta = 2$. Table 3 shows the first five natural frequency parameters for a cross-ply $[0/90]_3$ cylindrical panel as computed with ESL and LW theories of increasing order. The same analysis is carried out in Table 4 but for an angle-ply $[45/-45]_3$ panel. Present 2-D results are compared with those arising from a high-fidelity 3-D finite element analysis [19], which is assumed to be highly reliable. It is worth noting that ESL theories are rather inaccurate in both cases and for all frequencies under study, including the fundamental one. Increasing the order N of the ESL theory slightly improves the estimation, but the discrepancy between EDN and 3-D results is still significant even when $N = 6$ is adopted. The smallest difference in the results of EDN theories occurs in the fundamental frequency

Table 2: Non-dimensional frequency parameters $\lambda = \omega a \sqrt{\frac{\rho}{E}}$ of isotropic CCCC square spherical panels with $a/R_\alpha = 0.5$.

a/h	Theory	λ_1	λ_2	λ_3	λ_4	λ_5
10	ED4	1.2047	1.9451	1.9451	2.6956	3.1561
	[14]	1.1988	1.9301	1.9340	2.6828	3.1288
5	ED4	1.7625	2.8499	2.8499	3.7794	3.7794
	[14]	1.7405	2.8036	2.8091	3.7504	3.7572

Table 3: Non-dimensional frequency parameters $\lambda = \omega(a^2/h)\sqrt{\frac{\rho}{E_2}}$ of a $[0/90]_3$ CCCC cylindrical panel with $a/h = 10$ and $a/R_\beta = 2$.

Theory	λ_1	λ_2	λ_3	λ_4	λ_5
ED2	29.850	42.105	42.240	50.641	58.556
ED3	27.903	39.462	39.703	47.379	55.217
ED4	27.858	39.401	39.631	47.284	55.106
ED5	27.836	39.361	39.605	47.239	55.067
ED6	27.616	39.039	39.329	46.865	54.665
LD1	26.540	37.497	38.016	45.043	52.921
LD2	26.378	37.254	37.817	44.764	52.644
LD3	26.345	37.190	37.776	44.693	52.579
LD4	26.344	37.190	37.776	44.692	52.578
[19]	26.249	37.072	37.624	44.511	52.327

Table 4: Non-dimensional frequency parameters $\lambda = \omega(a^2/h)\sqrt{\frac{\rho}{E_2}}$ of a $[45/-45]_3$ CCCC cylindrical panel with $a/h = 10$ and $a/R_\beta = 2$.

Theory	λ_1	λ_2	λ_3	λ_4	λ_5
ED2	40.729	42.311	48.084	51.606	58.581
ED3	39.111	40.597	46.680	49.298	55.929
ED4	39.034	40.509	46.618	49.198	55.820
ED5	39.020	40.485	46.606	49.170	55.796
ED6	38.842	40.274	46.450	48.928	55.485
LD1	37.746	38.917	45.755	47.841	53.936
LD2	37.596	38.726	45.619	47.656	53.670
LD3	37.583	38.698	45.608	47.631	53.670
LD4	37.583	38.698	45.608	47.631	53.670
[19]	37.562	38.711	45.369	47.324	53.543

parameter λ_1 for the cross-ply lay-up wherein ED6 predicts a frequency 5.2% higher than 3-D analysis. A dramatic increase in accuracy is observed when 2-D layerwise theories are implemented. This is due to the capability by LW models of correctly predicting the through-the-thickness zig-zag behavior of the displacements in correspondence of each layer interface. The accuracy of LD1 is already acceptable with differences of about 1% with respect to 3-D models. If an improved accuracy is required, more costly higher-order LDN theories can be used.

Table 5 shows the same results as in the Table 3 for a CSCS cylindrical panel. A subset of ESL and LW models that can be implemented in the present modeling framework is selected. It can be seen again that the accuracy of EDN theories cannot be significantly improved beyond a certain limit by increasing the order N. Instead, LDN theories are capable of providing frequency parameters very close to 3-D values. As before, the degree of accuracy improves by using LW models of higher order.

In the last numerical example, a simply-supported SSSS square spherical panel is considered. It is composed of three layers oriented at $[0/90/0]$. The analysis is carried out for $a/h = 10$ and $a/h = 100$ (thin panel) and for different values of a/R_α including the plate case when $R_\alpha \to \infty$. The fundamental frequency parameter $\lambda = \omega(a^2/h)\sqrt{\frac{\rho}{E_2}}$

Table 5: Non-dimensional frequency parameters $\lambda = \omega(a^2/h)\sqrt{\frac{\rho}{E_2}}$ of a $[0/90]_3$ CSCS cylindrical panel with $a/h = 10$, $a/R_\beta = 2$.

Theory	λ_1	λ_2	λ_3	λ_4
ED2	17.449	27.266	34.854	39.118
ED3	16.869	25.570	33.439	36.701
ED4	16.847	25.528	33.390	36.623
LD1	16.465	24.336	32.493	34.961
LD2	16.411	24.181	32.372	34.752
[19]	16.338	24.020	32.222	34.513

is reported in Table 6 for each case. Comparison is provided with values from [24] where a layerwise approach is adopted in combination with a multiquadric radial basis function method. Results are in good agreement for both thin and thick case. In particular, it is shown that ESL models give very accurate predictions in the thin case without the need of relying on costly LW models.

5 Conclusions

An advanced modeling and solution framework for the prediction of natural frequencies of both thin and thick,

Table 6: Non-dimensional fundamental frequency parameters $\lambda = \omega(a^2/h)\sqrt{\frac{\rho}{E_2}}$ of [0/90/0] SSSS spherical panels.

a/h	Theory	a/R_α				
		0.2	0.1	0.05	0.02	0
10	ED2	12.7173	12.5723	12.5356	12.5253	12.5233
	ED3	11.9742	11.8112	11.7699	11.7583	11.7560
	ED4	11.9734	11.8108	11.7695	11.7580	11.7558
	LD1	11.8025	11.6362	11.5940	11.5822	11.5799
	LD2	11.6902	11.5214	11.4786	11.4665	11.4642
	LD3	11.6835	11.5146	11.4717	11.4597	11.4574
	[24]	11.8732	11.7072	11.6651	11.6533	11.6510
100	ED2	30.9955	20.3516	16.6334	15.4305	15.1905
	ED3	30.9873	20.3390	16.6180	15.4139	15.1736
	ED4	30.9829	20.3371	16.6173	15.4137	15.1736
	[24]	31.0402	20.4065	16.6969	15.6714	15.4349

deep and shallow cylindrical and spherical panels with different boundary conditions and arbitrary lamination lay-up is presented. The approach combines the capability of building hierarchically 2-D shell models based on equivalent single-layer and layerwise theories of variable order and the efficiency and simplicity of the spectral collocation solution method. The formulation is expressed in a compact matrix form which can be directly and easily coded in any modern mathematical software package. It has been shown through comparison with a fully 3-D analysis that stringent requirements on the accuracy of the computed frequency values can be satisfied only by 2-D high-order layerwise models, in particular when thick and deep anisotropic curved panels are considered. However, the present approach can also allow to build less costly low-order equivalent single-layer models when a more refined analysis is not required for the specific case under investigation.

$$\left(J^{k\tau_z s}, J^{k\tau_z s}_\alpha, J^{k\tau_z s}_\beta\right) = \int_{z_k} \frac{\partial F_\tau}{\partial z} F_s \left(1, H^k_\alpha, H^k_\beta\right) dz$$

$$\left(J^{k\tau_z s}_{\alpha/\beta}, J^{k\tau_z s}_{\beta/\alpha}, J^{k\tau_z s}_{\alpha\beta}\right) = \int_{z_k} \frac{\partial F_\tau}{\partial z} F_s \left(\frac{H^k_\alpha}{H^k_\beta}, \frac{H^k_\beta}{H^k_\alpha}, H^k_\alpha H^k_\beta\right) dz$$

$$\left(J^{k\tau s_z}, J^{k\tau s_z}_\alpha, J^{k\tau s_z}_\beta\right) = \int_{z_k} F_\tau \frac{\partial F_s}{\partial z} \left(1, H^k_\alpha, H^k_\beta\right) dz$$

$$\left(J^{k\tau s_z}_{\alpha/\beta}, J^{k\tau s_z}_{\beta/\alpha}, J^{k\tau s_z}_{\alpha\beta}\right) = \int_{z_k} F_\tau \frac{\partial F_s}{\partial z} \left(\frac{H^k_\alpha}{H^k_\beta}, \frac{H^k_\beta}{H^k_\alpha}, H^k_\alpha H^k_\beta\right) dz$$

$$\left(J^{k\tau_z s_z}, J^{k\tau_z s_z}_\alpha, J^{k\tau_z s_z}_\beta\right) = \int_{z_k} \frac{\partial F_\tau}{\partial z} \frac{\partial F_s}{\partial z} \left(1, H^k_\alpha, H^k_\beta\right) dz$$

$$\left(J^{k\tau_z s_z}_{\alpha/\beta}, J^{k\tau_z s_z}_{\beta/\alpha}, J^{k\tau_z s_z}_{\alpha\beta}\right) = \int_{z_k} \frac{\partial F_\tau}{\partial z} \frac{\partial F_s}{\partial z} \left(\frac{H^k_\alpha}{H^k_\beta}, \frac{H^k_\beta}{H^k_\alpha}, H^k_\alpha H^k_\beta\right) dz$$

Appendix

The thickness integrals in the fundamental nuclei $\mathbf{K}^{k\tau s}_{ij}$, $\mathbf{M}^{k\tau s}_{ij}$, and $\mathbf{B}^{k\tau s}_{ij}$ of the present formulation are defined as follows:

$$\left(J^{k\tau s}, J^{k\tau s}_\alpha, J^{k\tau s}_\beta\right) = \int_{z_k} F_\tau F_s \left(1, H^k_\alpha, H^k_\beta\right) dz$$

$$\left(J^{k\tau s}_{\alpha/\beta}, J^{k\tau s}_{\beta/\alpha}, J^{k\tau s}_{\alpha\beta}\right) = \int_{z_k} F_\tau F_s \left(\frac{H^k_\alpha}{H^k_\beta}, \frac{H^k_\beta}{H^k_\alpha}, H^k_\alpha H^k_\beta\right) dz$$

References

[1] V.V. Novozhilov, *Thin shell theory*, P. Noordhoff, 1964.

[2] H. Kraus, *Thin elastic shells*, John Wiley & Sons, 1967.

[3] E. Ventsel, T. Krauthammer, *Thin plates and shells*, Marcel Dekker, 2001.

[4] W. Soedel, *Vibration of shells and plates*, Marcel Dekker, 2004.

[5] A.W. Leissa, Vibration of shells, NASA-SP-288, 1973.

[6] K.M. Liew, S. Kitipornchai, C.M. Wang, Vibration of shallow shells: A review with bibliography, *Applied Mechanics Review*, 50, 1997, 431-444.

[7] M.S. Qatu, Recent research advances in the dynamic behavior of shells: 1989-2000, Part 2: Homogeneous shells, *Applied Mechanics Review*, 55 (2002), 415-434.

[8] A.K. Noor, W.S. Burton, Assessment of computational models for multilayered composite shells, *Applied Mechanics Review*, 43 (1990), 67-97.

[9] M.S. Qatu, Recent research advances in the dynamic behavior of shells: 1989-2000, Part 1: Laminated composite shells, *Applied Mechanics Review*, 55 (2002), 415-434.

[10] L. Meirovitch, *Computational methods in structural dynamics*, Sijthoff & Noordhoff, 1980.

[11] A.W. Leissa, M.S. Qatu, *Vibration of continuous systems*, McGraw-Hill, 2011.

[12] K.P. Soldatos, V.P. Hadjigeorgiou, Three-dimensional solution of the free vibration problem of homogeneous isotropic cylindrical shells and panels, *Journal of Sound and Vibration*, 137 (1990), 369-384.

[13] J. Ye, K.P. Soldatos, Three-dimensional vibration of laminated cylinders and cylindrical panels with symmetric or antisymmetric cross-ply lay-up, *Composites Engineering*, 4 (1994), 429-444.

[14] K.M. Liew, L.X. Peng, T.Y. Ng, Three-dimensional vibration analysis of spherical shell panels subjected to different boundary conditions, *International Journal of Mechanical Sciences*, 44 (2002), 2103-2117.

[15] E. Asadi, W. Wang, M.S. Qatu, Static and vibration analyses of thick deep laminated cylindrical shells using 3D and various shear deformation theories, *Composite Structures*, 94 (2012), 494-500.

[16] E. Carrera, Theories and finite elements for multilayered plates and shells: a unified compact formulation with numerical assessment and benchmarking, *Archives of Computational Methods in Engineering*, 10 (2003), 215-296.

[17] K.M. Liew, X. Zhao, A.J.M. Ferreira, A review of mesh less methods for laminated and functionally graded plates and shells, *Composite Structures*, 93 (2011), 2031-2041.

[18] F. Tornabene, 2-D GDQ solution for free vibrations of anisotropic doubly-curved shells and panels of revolution, *Composite Structures*, 93 (2011), 1854-1876.

[19] E. Asadi, M.S. Qatu, Free vibration of thick laminated cylindrical shells with different boundary conditions using general differential quadrature, *Journal of Vibration and Control*, 19 (2012), 356-366.

[20] F. Tornabene, E. Viola, N. Fantuzzi, General higher-order equivalent single layer theory for free vibrations of doubly-curved laminated composite shells and panels, *Composite Structures*, 104 (2013), 94-117.

[21] E. Carrera, Layer-wise mixed models for accurate vibration analysis of multilayered plates, *Journal of Applied Mechanics*, 65 (1998), 820-828.

[22] C. Canuto, M.Y. Hussaini, A. Quarteroni, T.A. Zang, *Spectral Methods - Fundamentals in Single Domains*, Springer, Berlin, 2006.

[23] B. Fornberg, *A Practical Guide to Pseudospectral Methods*, Cambridge University Press, 1996.

[24] A.J.M Ferreira, E. Carrera, M. Cinefra, C.M.C. Roque, Analysis of laminated doubly-curved shells by a layerwise theory and radial basis functions collocation, accounting for through-the-thickness deformation, *Computational Mechanics*, 48 (2011), 13-25.

[25] F.A. Fazzolari, E. Carrera, Advances in the Ritz formulation for free vibration response of doubly-curved anisotropic laminated composite shallow and deep shells, *Composite Structures*, 101 (2013), 111-128.

[26] L. Dozio, E. Carrera, A variable kinematic Ritz formulation for vibration study of quadrilateral plates with arbitrary thickness, *Journal of Sound and Vibration*, 330 (2011), 4611-4632.

[27] L. Dozio, E. Carrera, Ritz analysis of vibrating rectangular and skew multilayered plates based on advanced variable-kinematic models, *Composite Structures*, 94 (2012), 2118-2128.

[28] L. Dozio, Natural frequencies of sandwich plates with FGM core via variable-kinematic 2-D Ritz models, *Composite Structures*, 96 (2013), 561-568.

[29] J.N. Reddy, *Mechanics of Laminated Composite Plates and Shells: Theory and Analysis*, CRC Press, 2004.

[30] J.A.C. Weideman, S.C. Reddy, A MATLAB differentiation matrix suite, *ACM Transactions on Mathematical Software*, 26 (2000), 465-519.